ADVANCES IN ATMOSPHERIC SCIENCES, VOL. 26, NO. 6, 2009, 1169–1180

Correlation Analysis of Persistent Heavy Rainfall Events in the Vicinity of the Yangtze River Valley and Global Outgoing Longwave Radiation in the Preceding Month

TANG Yanbing*[1] (汤燕冰), ZHAO Lu[2] (赵 璐), and GAO Kun[1] (高 坤)

[1] *Department of Earth Sciences, Zhejiang University, Hangzhou* 310027

[2] *Zhejiang Meteorological Observatory, Hangzhou* 310017

(Received 7 January 2008; revised 25 January 2009)

ABSTRACT

Based on the National Oceanic and Atmospheric Administration (NOAA) daily satellite dataset of global outgoing longwave radiation (OLR) for the period of 1974–2004 and the NCEP-NCAR reanalysis for 1971–2004, the linkage between persistent heavy rainfall (PHR) events in the vicinity of the Yangtze River valley and global OLR leading up to those events (with 1- to 30-day lag) was investigated. The results reveal that there is a significant connection between the initiation of PHR events over the study area and anomalous convective activity over the tropical Indian Ocean, maritime continent, and tropical western Pacific Ocean. During the 30-day period prior to the onset of PHR events, the major significantly anomalous convective centers have an apparent dipole structure, always with enhanced convection in the west and suppressed convection in the east. This dipole structure continuously shifts eastward with time during the 30-day lead period. The influence of the anomalous convective activity over the tropical oceans on the initiation of PHR events over the study area is achieved via an interaction between tropical and extratropical latitudes. More specifically, anomalous convective activity weakens the Walker circulation cell over the tropical Indian Ocean first. This is followed by a weakening of the Indian summer monsoon background state and the excitation and dispersion of Rossby wave activity over Eurasia. Finally, a major modulation of the large scale background circulation occurs. As a result, the condition of a phase-lock among major large scale circulation features favoring PHR events is established over the study area.

Key words: persistent heavy rainfall events, global outgoing longwave radiation, the Yangtze River valley

Citation: Tang, Y. B., L. Zhao, and K. Gao, 2009: Correlation analysis of persistent heavy rainfall events in the vicinity of the Yangtze River valley and global outgoing longwave radiation in the preceding month. *Adv. Atmos. Sci.*, **26**(6), 1169–1180, doi: 10.1007/s00376-009-8006-x.

1. Introduction

Persistent heavy rainfall events (hereafter, PHR events), which are characterized by high intensity, broad extent, and persistence, are one category of weather- and climate-related extreme precipitation events. Affected by the Asian monsoon system, PHR events represent a climate feature of East Asia. Most severe floods in China, especially in the Yangtze River valley, are caused by this type of extreme, for example, the flood disasters in the Yangtze River valley in 1991, 1998, and 1999 (Zhang et al., 2002). Such extreme events can cause great costs to society through damage to property, loss of life, and disruption of shipping, aviation, energy management, and agriculture. The skillful prediction of PHR events remains one of the greatest scientific and societal challenges of the 21st century.

THORpex (THe Observing system Research and predictability experiment) aims to accelerate improvements in medium-range (3 to 7 days) and extended-range (week two) weather predictions and improve forecasts of related high-impact weather. Poor forecasts of such extreme events increase their societal and economic impact. On the other hand, improved forecasts will help mitigate these losses by providing gov-

*Corresponding author: TANG Yanbing, y_tang@zju.edu.cn

ernment agencies, the general public, and businesses with more accurate warnings (Shapiro and Thorpe, 2002). With the consideration of the long duration, broad extent, and high intensity, proper forecasting for PHR events should be a corresponding medium range forecasting issue for about 1–3-week lead or more. It is clear that such extreme events must be a result of long-brewed steady circulation backgrounds. However, the formation and persistence of such favorable circulation background states greatly depends on the interaction of many factors with different spatial and temporal scales. These factors include, for example, heating over the surface, the behavior of tropical convection, and the adjustment of related circulation features.

Satellites are important sources for obtaining data, especially over areas where conventional data are limited or even unavailable. Moreover, the broad spatial coverage and long period of records have also made satellite data invaluable in investigating atmospheric phenomena with a variety of temporal and spatial scales (Heddinghause and Krueger, 1981; Lau and Chan, 1983; Wang, 1994; Wang and Xu, 1997; Xie and Arkin, 1998). Outgoing longwave radiation (OLR) estimates have been made since 1974 from the window channel measurements of the operational National Oceanographic and Atmospheric Administration (NOAA) polar-orbiting satellites (Gruber and Krueger, 1984). The flux of OLR is dominated by two factors: clouds and surface temperatures. Regions of intense frequent convection appear as low OLR regions (Chelliah and Arkin, 1992). OLR can offer reasonably good estimates for deep convection and rainfall in most tropical and prevailing monsoon regions (Li et al., 2004).

Many studies have been devoted to linkages between rainfall in China and the behavior of OLR (Jiang and Winston, 1989; Li and Liu, 1990; Shi and Zhu, 1991; Jiang et al., 1993; Li et al., 2004). However, most of these focus on the linkages either on long time scales (monthly or annual) or short scales (0–3 days). Less attention has been paid to the scale between monthly and daily scales, which is critical to medium range forecasting. Besides, research on connections between behavior of global OLR and extreme precipitation events, such as PHR events, is still limited. Therefore, the objective of this study is to identify possible connections between global OLR anomalies and the initiation and evolution of PHR events over the vicinity of the Yangtze River valley, since this region is most vulnerable to PHR events (Tang et al., 2006). In other words, this study will try to find where and when significant anomalies of OLR have substantial influences on the initiations of subsequent PHR events. For convenience, the OLR signals are defined as clusters of long-lived OLR anomalies, which are significantly associated with PHR events.

The data and methods used in this study are described in section 2. Section 3 presents the study results, and major conclusions are provided in section 4.

2. Data and methods

2.1 *Data*

The daily mean OLR data used in this study were provided by NOAA CDC (Climate Diagnostics Center), on a global grid of $2.5^\circ \times 2.5^\circ$, from 1 June 1974 to 30 November 2004 (except for 1978 due to satellite failure). The corresponding OLR daily long-term mean was based on the period of 1979–1995. Standardized OLR anomalies (SOLRA hereafter) were computed as the basic variable to which different meteorological elements in further study are referenced.

The daily averaged circulation fields, including geopotential height and both flow components, for the period from 1971 to 2004 were from NCEP-NCAR reanalysis. The climatic mean was constructed by averaging values on individual days of the year over the 30-yr period 1971–2000.

The precipitation data used in this study consist of daily totals from 743 observation stations operating in China during the period of 1974–2004, and a gridded dataset of summer (April–August) daily rainfall was constructed by interpolating all available station records for a given day into 30 km by 30 km grid boxes within China.

2.2 *Cases and methodology*

Based on a previous study (Tang et al., 2006), eight severe PHR events occurring in the vicinity of Yangtze River valley under westerly flow regimes were selected as PHR event cases. Of these events, one case was in the 1970s, one in the 1980s, four in 1990s, and two after the year 2000. All eight cases occurred in late June and the average onset date is 25 June. Additionally, these event cases share a long average duration of about 10.4 days.

For comparison, eight null event cases were also defined. As with the PHR event cases, the null cases were selected from either June or July. The length of a null case was at least seven days, which is the minimum length of the selected extreme rainfall event cases for this study. During these seven days, there was either no precipitation at all or only scattered precipitation over the study area. Of all eight null cases, one occurred in the 1970s, four in the 1980s, two in the 1990s, and one after the year 2000. Therefore, the eight PHR event cases and eight null cases compose the case pop-

ulation for lag-correlation computation and analysis.

To facilitate further analysis, areal rainfall (AR) was defined as an indicator to depict the features of PHR events. AR (10^3 mm km^2) was defined as the area-weighted sum of the total rainfall over the event rainband during the period of event. The event rainband in this study was defined as the area of contiguous grid cells that received more than 100 mm precipitation over the duration of the event. AR can be used to describe the intensity of event. Given events with an equal persistent rainfall duration, a higher value of AR would result from either more intense precipitation and/or a broader extent of the event. The averaged AR value for event cases is 107708.8 ($\times 10^3$ mm km^2), and the mean AR is only 2528.4 ($\times 10^3$ mm km^2) for null cases.

As mentioned previously, this study is mainly interested in identifying possible signals of global OLR which are strongly related to the initiation and evolution of PHR events over the medium range (3 to 14 days). However, considering the complexity of impacts on the PHR events and our limited knowledge about linkages between global OLR and the initiation of the PHR events, the investigation period was extended to 1 to 30 days instead of just 3 to 14 days before the onset time of the PHR events.

Lag-correlations were computed between AR values of both event and null cases and global SOLRA fields each day from day−30 (i.e., 30 days prior to the onset date of the events) to day−1. Moreover, Monte Carlo testing technique was used for the significance testing of lag correlation coefficients in this study, since there is no constraint of normality required (Livezey and Chen, 1983; Shi et al., 1997). The statistical confidence level employed is above 90%.

It should be pointed out that all significant lag-correlation coefficients beyond 40°N/40°S were discarded, because only in relatively low-latitude areas is OLR mostly modulated by cloudiness alone (Heddinghause and Krueger, 1981), and thus properly reflecting convective activity as desired.

3. Results

3.1 *Identification of the OLR signals*

From the frequency distribution of significant daily lag-correlation results, there are several high frequency centers, which correspond to areas with significant positive or negative correlations. The major significant daily positive correlation areas are around the maritime continent and Philippine Sea, and major negative correlation areas are in the tropical western Indian Ocean. Compared to the daily distribution of composite SOLRA of the event cases, it is obvious that the composite SOLRA fields for day−30 to day−1 correspond well with the correlation fields. Generally, negative SOLRA are accompanied by significant negative correlations and positive SOLRA by positive correlations. Since this study aims at investigating the connection between anomalous OLR and PHR events, only these two situations (either negative SOLRA accompanied by significant negative correlations or positive SOLRA by significant positive correlations) were considered. These two situations were defined as negative and positive OLR signals, respectively, for this study. Although the signs of both kinds of OLR signals are different, their meanings are the same. That is, both kinds of signals suggest that the convective activities related to these signals favor the initiation and development of subsequent PHR events.

Along with the characteristics of the PHR events mentioned above, attention was paid to the relatively stable SOLRA areas with significant correlation coefficients. The primary criteria for choosing OLR signals were as follows:

(1) The areas with significant correlation coefficients should also be areas with significant SOLRA for the composite of PHR event cases. The threshold for significant SOLRA is either >0.3 or < -0.3 for this study.

(2) The area that meets the first criterion should be relatively stable. If not, its daily variation should be continuous.

(3) Significant SOLRA and correlation must be maintained for more than 4 days.

(4) There should be major differences in SOLRA between the composites of rain PHR event cases and null cases in the area during the duration of significant SOLRA and correlation.

Following these criteria, many OLR signals were primarily identified. However, some of them might not really be important, or may not have much physical meaning. As mentioned above, the OLR signal appearing preceding PHR events should have significant influence on the development and evolution of the subsequent PHR events. Therefore, the OLR signals were further identified.

Signal intensity (SI) was defined as an indicator to depict the intensity feature of OLR signals, using Eq. (1). SI was calculated as the latitude-weighted sum of SOLRA grid values in the duration of an OLR signal.

$$\mathrm{SI} = \sum_t \sum_i S_{t,i} \cdot \cos \varphi_{t,i} \ , \qquad (1)$$

where the sum is performed for all proper grid cells located in the signal. $S_{t,i}$ is the SOLRA value over

the i-th grid cell; $\cos\varphi_{t,i}$ is the corresponding cosine latitude value of the grid cell; i runs over the grid cells inside the signal, and t is the length (days) of the signal. Multiplying by $\cos\varphi_{t,i}$ adjusts the area weighting based on the map projection with the increase of latitude. It should be clarified that only positive OLR values are qualified for summing for positive signals, and negative OLR values for negative signals. SI can be used to describe the intensity of individual OLR signals. Given signals with an equal duration, a higher value of SI would result from either more intense SOLRA and/or a bigger scope of the signal.

The linear correlation coefficient between the SI series and AR series for each OLR signal was computed. Then, only those signals with significant correlation coefficients at the 95% confidence level were selected for further analysis.

3.2 *An overview of the signals found*

Figure 1 shows the composite SOLRA averaged from day−30 to day−1 based on 8 rainfall PHR event cases, and the tracks of significant positive and negative OLRA centers in each pentad within the 30-day period before the PHR events. It can be seen from Fig. 1 that significant negative SOLRA, which denotes enhanced convection, mainly cluster in the western tropical Indian Ocean, and significant positive SOLRA, which denote suppressed convection, gather on the eastern tropical Indian Ocean, the maritime continent, and the western North Pacific Ocean. Compared to the enhanced convection centers clustered in the zone from 5°N to 10°N, the suppressed convection centers spread from 10°S to 20°N in three east-west orientation clusters. One important point to note is that the

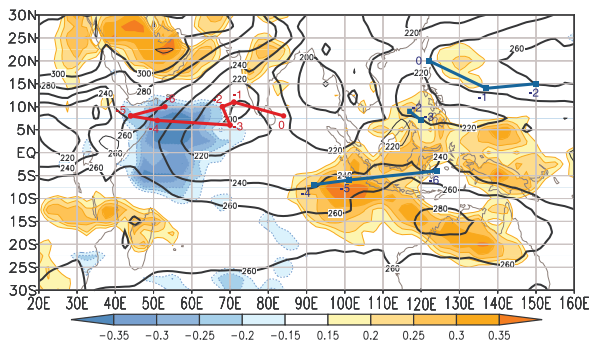

Fig. 1. Composite of SOLRA (shaded) and OLR (contoured with interval of 20 W m^{-2}) averaged from day−30 to day−1. The blue squares and red circles denote the significant negative and positive OLRA centers identified for each pentad during the period from day−30 to day+4. The heavy solid lines indicate the traces of both positive and negative OLR anomaly centers according to the time order, from −6 to 0.

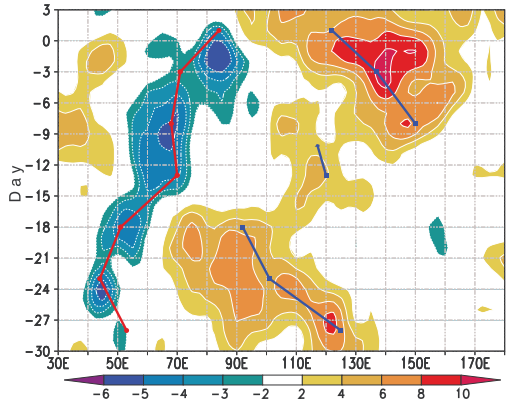

Fig. 2. Time-longitude plot of composite areas with significant SOLRA over the zones between 0° and 15°N for negative SOLRA, and between 13°S and 25°N for positive SOLRA. The areas are defined by the sums of grids with absolute values of SOLRA above 0.3 in corresponding zones. The solid (dashed) contour indicates the area having significant positive (negative) correlation (above 90% confidence level) with the PHR events. The blue squares and red circles as well as the connecting lines between them have the same meanings as in Fig. 1.

anomalous convective centers have an apparent dipole structure, always with the anomalously enhanced convection in the west and anomalously suppressed convection in the east, as shown in Fig. 1.

Figure 2 is a time-longitude diagram of the significant SOLRA averaged over the zone between 0°N and 15°N for the negative SOLRA, and between 13°S and 25°N for the positive SOLRA, respectively. It is obvious that both clusters of the significant negative and positive SOLRA move eastward with a prominent dipole structure with time. In contrast to the continuously eastward propagation of the dipole structure and enhanced convection centers, there are three pronounced westward propagation sequences of the suppressed convection centers with positive SOLRA over the maritime continent and the western Pacific during the period. It is noted that these three westward propagations of suppressed convection centers occur in the three east-west orientation clusters, respectively (Fig. 1). As shown in Fig. 2, the first westward propagation of the suppressed convection center from the maritime continent to the central tropical Indian occurs during the time period from day−30 to day−15. Then, the suppressed convection center westward propagation within the maritime continent follows. Finally, the suppressed convection center shifts westward from the western Pacific to the maritime continent 10 days before the onset of PHR events. It is clear that the behavior of the SOLRA during the period of 30 days before the PHR events manifest the activities of the

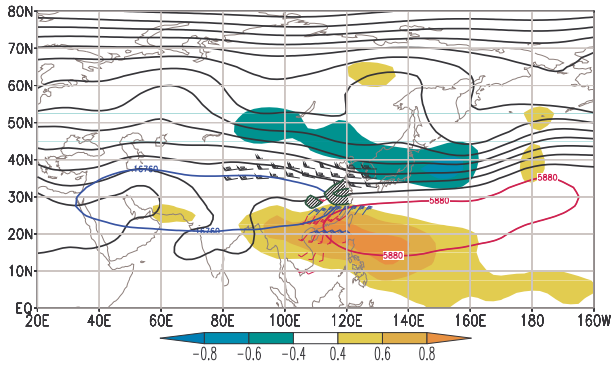

Fig. 3. Composite of mean large scale circulation background for the period from the onset day to day+4 of the PHR events based on eight event cases. The black lines are contours of geopotential height at 500 hPa and the contour interval is 20 m. The shaded areas indicate significant geopotential height anomalies at the same level. The blue line represents the location of the SAH at 100 hPa. The red wind barbs represent significant (above 90% statistical confidence level) winds at 850 hPa, black at 200 hPa, and blue at 100 hPa respectively. The green lines indicate the position of rainbands for PHR events over the study area.

dominant patterns of intraseasonal variability over the Asian summer monsoon domain (Annamalai and Slingo, 2001; Wang et al., 2001; Lawrence and Webster, 2002; Ding and Chan, 2005).

3.3 *The large scale circulation background of the PHR events*

To explore the relationship between the signals and large scale circulation features originating the PHR events, it is necessary to present the large scale circulation background for the duration of PHR events. Figure 3 is a schematic diagram of the composite large scale circulation background averaged over the first seven days of eight PHR event cases. As shown in Fig. 3, the major circulation features include the South Asian High (SAH) in the upper troposphere, the Subtropical Western Pacific High (SWPH) and the Okhotsk blocking high in the mid troposphere, as well as both high and low level jets in the lower and upper troposphere, respectively. PHR events occur under the conditions of a phase-lock among these major large scale circulation features at different latitudes, and over different levels.

The most salient circulation feature for the phase-lock condition is the SWPH in the lower and mid troposphere. Accompanied with the significant positive height anomaly at 500 hPa as shown in Fig. 3, the SWPH is encompassed by the 5 880 m contour of geopotential, which extends westward to 110°E, and is in favor of the establishment of persistent rainbands along its northwest periphery over the Yangtze River-Huaihe River valleys (Samel et al., 1999; Ding and Chan, 2005). Conversely, the SAH as encompassed by the 16 760 m contour extends eastward to 115°E in the upper troposphere. Between them, a strong lower level southwesterly jet, which extends to 400 hPa (not shown), builds up on the west flank of the SWPH, and a strong upper level northeasterly flow occurs on the east flank of the SAH. Therefore, a local secondary meridional circulation (a so-called monsoon circulation cell, Ding and Chan, 2005) is formed with northeasterly flow in the upper level and southwesterly flow at the lower levels. The strong upward motion of this monsoon circulation cell corresponds well with the heavy rainband. At the same time, the upper level westerly jet locates in the zone between 30°N and 40°N and stretches from 80°E to 130°E, thus leading to intensification of upper level divergence on its south flank, which greatly favors low level northward moisture transport and convergence in the study area.

On the other hand, a dual blocking high situation, with a relatively weak one over the Ural Mountains and a strong one over the Okhotsk Sea, is established in the mid and high latitudes. It should be pointed out that there is a significant negative height anomaly belt stretching from western Mongolia to the North Pacific east of Japan with a WNW–ESE (West-North-West–East-South-East) orientation. This implies that minor troughs frequently travel east-southeastward during PHR events. These minor troughs advect weak cold dry air and meet warm moist air from the south over the study area, sharpening the thermal gradient and intensifying convective activity there (Samel et al., 1999; Ding and Chan, 2005).

3.4 *Relationship between the OLR signals and large scale circulation features associated with PHR events*

As shown in Fig. 2, the anomalous convection has an east/suppressed-west/enhanced pattern over the tropical Indian and western North Pacific Oceans within the period of 30 days before the onset of PHR events. Normally, the Walker circulation cell over the Indian Ocean has its rising branch extending from the eastern tropical Indian Ocean to the maritime continent and its sinking branch over the area off the Somalian coast (not shown). In respond to this anomalous dipole heating pattern, the Walker circulation cell over the Indian would be weakened. As is well known, the Walker circulation is one of the large-scale systems observed in the near equatorial atmosphere and changes in this circulation can have far-reaching consequences (Pierrehumbert and Benestad, 2006). Among these consequences, this study focuses on how the anoma-

lous Walker circulation, which is denoted by the signals, modulates the evolution of the large scale circulation to generate the phase-lock condition for the duration of the PHR events mentioned above.

To investigate the relationship between the convective signals and the related large scale circulation features, a feasible approach was designed according to the behavior of OLR signals mentioned above. The approach includes two methods, a simple correlation analysis and composite analysis. The former was conducted based on the 54-yr circulation fields, including geopotential height and both flow components, derived from NCEP/NCAR reanalyses. According to the onset dates of the eight event cases, the seven pentads from late May to late June, which corresponds with the time period 30 days before and 5 days after the onset of PHR events, were defined for correlation analysis. A "one-point" correlation map of pentad averaged circulation fields with reference to the OLR signal identified in the same pentad was designed to illustrate the significant connection between the anomalous OLR and circulation fields. The latter was based on 8 event cases. The six pentad-mean composite circulation fields were derived to demonstrate the evolution of anomalous circulation during the period 30 days prior to the onset of PHR events.

3.4.1 *A weakening Indian summer monsoon (ISM) background for the PHR events*

As mentioned above, the anomalous coherent changes in the convection pattern over the Asian summer monsoon domain have substantial impacts on the general circulation. The east-suppressed/west-enhanced anomalous convection pattern weakens the Walker circulation cell over the tropical Indian. Figure 4 shows a "one-point" correlation map for the first pentad of June (approximately the period from day−25 to day−21). During this five day period, the anomalous enhanced convection is over the area off the Somali coast, while the suppressed area is offshore of the southwest coast of Sumatra. In respond to this anomalous heating pattern, an anomalous anti-cyclonic flow appears over the Indian peninsula and Bay of Bengal in the lower and mid troposphere. This suggests the weakening of the Indian monsoon low. As expected, anomalous easterlies extend from the Bay of Bengal to the Arabian Sea at 850 hPa. It is obvious that this response of circulation features manifests a weakening ISM condition in the low and mid troposphere. A similar situation also appears in other pentads. This implies that anomalous convective activities characterized by the west-enhanced/east-suppressed pattern over the tropical Indian and maritime continent are favorable for a weakening ISM. Therefore, it is obvious

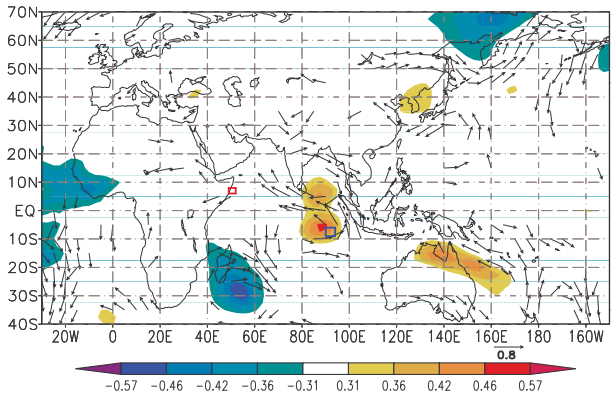

Fig. 4. "One point" correlation map showing the correlation coefficient between the magnitude difference of OLR pairs at two base points (shown as red and blue boxes) and the pentad averaged height as well as wind fields at 850 hPa for the first pentad of June from 1974 to 2004. The values above 90% statistical confidence level are shaded for height and plotted for wind vectors.

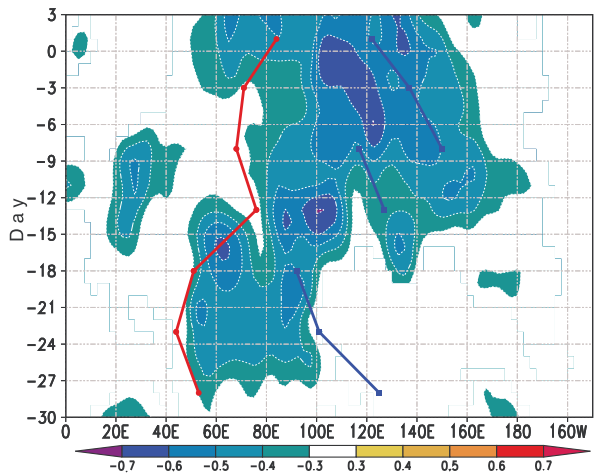

Fig. 5. Time-longitude plot of composite normalized zonal wind negative anomalies averaged between 0° and 10°N at 850 hPa for the 8 PHR events. The blue squares and red circles as well as the connecting lines between them have the same meanings as in Fig. 1.

that a direct consequence of the weakening Walker cell is the occurrence of a weak Indian summer monsoon condition.

The relationship between OLR and pentad-averaged circulation features revealed by "one-point" correlation maps is also shown in the composite anomaly fields. Figure 5 is a time-longitude plot of composite zonal wind anomalies averaged between 0° and 10°N at 850 hPa for the 8 PHR events. It is clear in Fig. 5 that the reduced westerlies shifts eastward

in the low troposphere with the eastward shift of the pair of anomalous convection centers. Additionally, significant easterly anomalies prevail from the Indian peninsula to the Arabian Sea and northerlies along the Somali coast (not shown). In contrast to the lower levels, significant upper level westerlies extends from the Somali coast and Arabian Sea to the Indian peninsula, weakening the subtropical easterly jet. All of these factors suggest not only the existence of a weakened Walker circulation cell over the tropical Indian, but a weakened ISM as well. The weakened Walker cell and reduced cross-equator flow along the Somali coast are tied to the anomalous convective activity manifest in a weakened ISM background before onset of PHR events. It should be pointed out that a weak ISM is an important characteristic for the large scale background favoring PHR events (Lau and Li, 1984; Zhang et al., 2002; Ding and Chan, 2005; Ding, 2005).

3.4.2 *The activities of the Rossby wave train prior to the PHR events*

The most salient feature demonstrated in both of the "one point" correlation maps and the composite anomaly circulation fields is the signature of a significant Rossby wave train in the troposphere, especially in the upper level flow. A number of previous studies have revealed that anomalous adiabatic heating resulting from abnormal convective activities over the tropical Indian Ocean will generate a source of Rossby wave activity that can propagate into the mid-latitudes (Lau and Li, 1984; Wang, 1994; Wang et al., 2001; Annamalai and Slingo, 2001; Ding, 2005; Ding and Chan, 2005; Ding and Wang, 2005, 2007; Iwao and Takahashi, 2008).

The Rossby wave activity is significantly associated with the establishment of the large scale phase-lock condition, and starts about 2 weeks before the PHR events. Figure 6a is a "one point" correlation map for the third pentad of June at 150 hPa. It can be seen from Fig. 6a that there is a significant correlation between the development of an anomalous low centered around the Aral Sea and anomalously enhanced convection over the Indian Ocean southwest of the Indochina Peninsula. On the western side of the anomalous low, strong anomalous northerly flow extends from European Russia to Saudi Arabia. Conversely, strong southerly and southwesterly flow extends from the Arabian Sea to central Siberia on the eastern side of the low. Additionally, another two significant cyclonic flows are located over the northern African continent and southeast China, respectively. The relationship between the anomalous convection and upper level circulation features indicated by the "one point" correlation map is consistent with the

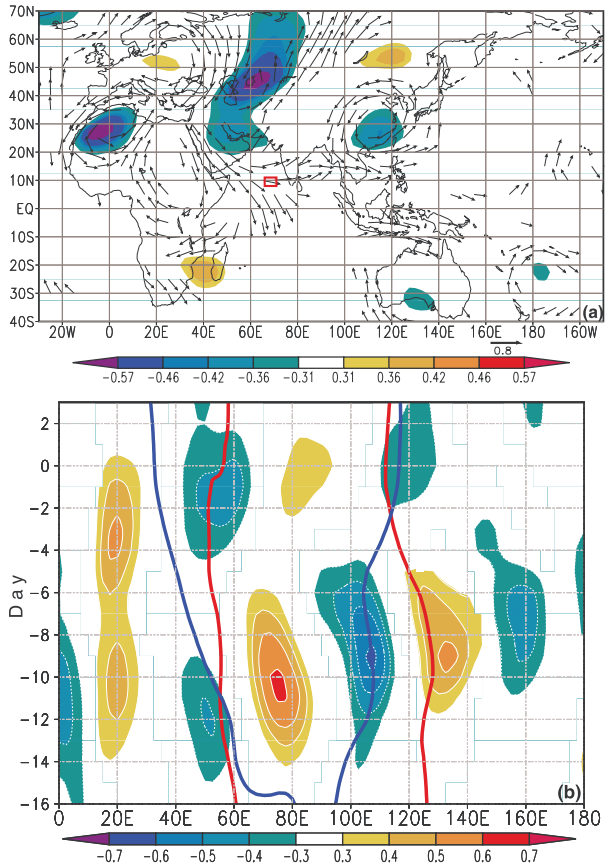

Fig. 6. (a) "One point" correlation map showing the correlation coefficient between the OLR at a base point (shown as red rectangle) and the pentad averaged height as well as wind fields at 150 hPa for the third pentad of June from 1974 to 2004. The values above the 90% statistical confidence level are shaded for height and plotted for wind vectors. (b) Time-longitude plot of composite meridional wind anomalies averaged over the zone between 25°N and 45°N at 150 hPa for the 8 PHR events. The blue thick line is the contour of 16760 m showing the averaged height at 100 hPa from 25°N to 30°N and the red line is for 5880 m at 500 hPa from 15°N to 25°N.

situation shown by the composite of eight PHR events. Figure 6b is a time-longitude chart of anomalous meridional wind averaged between 25°N and 45°N at 150 hPa. It is clear in Fig. 6b that significant meridional wind anomalies are closely associated with the PHR events and manifest a Rossby wave train during the period from day−15 to day−5. The three anomalous troughs locate correspondingly around 60°E, 120°E, and 180°E, which match well with the cyclonic flows over the Aral Sea and southeast China, respectively shown in Fig. 6a. These centers correspond well with the action centers of a recurrent circumglobal teleconnection (CGT) pattern in the summertime mid latitude circulation of the North-

ern Hemisphere. The CGT is a source of climate variability and predictability in the mid latitude regions of the Northern Hemisphere in summer (Ding and Wang, 2005, 2007).

With the southeastward dispersion of this Rossby wave train, the large scale circulation undergoes a major modulation, which is clearly demonstrated in Fig. 7. Figure 7 is the composite anomalous flow at 150 hPa from day−13 to day−3. At day−13, a pair of upper level height anomalies appears over Eurasia with a negative center around western Siberia and a positive center around Baikal (Fig. 7a), corresponding to significantly anomalous meridional flows over 50°E, 75°E, and 105°E respectively (Fig. 7b). With the southeastward dispersion of the wave train, significant southerly flow develops over 130°E (Fig. 6b), and an anomalous low appears over southeast China at day−10 (Fig. 7b). At the same time, the anomalous high around the Baikal region breaks into two parts. One part shifts eastward to the vicinity of the Okhotsk Sea and intensifies the ridge in the climatological basic flow there. The other part intensifies over the northeastern part of the Tibetan Plateau, which is favorable for the northward expansion of the SAH. At day−7, the anomalous low over southeast China is further enhanced, responding to two abnormal suppressed convection centers over the Philippine Sea (see Figs. 1 and 7c). Also, it can be seen in Fig. 7c that alternating anomalous lows and highs develop downstream along the subtropical westerly jet, which intensifies the ridge over the Okhotsk Sea and deepens the trough over the central North Pacific. Then, the anomalous low over southeast China weakens and a long wave trough develops over the Baikal with the disappearance of the Rossby wave train (Fig. 7d).

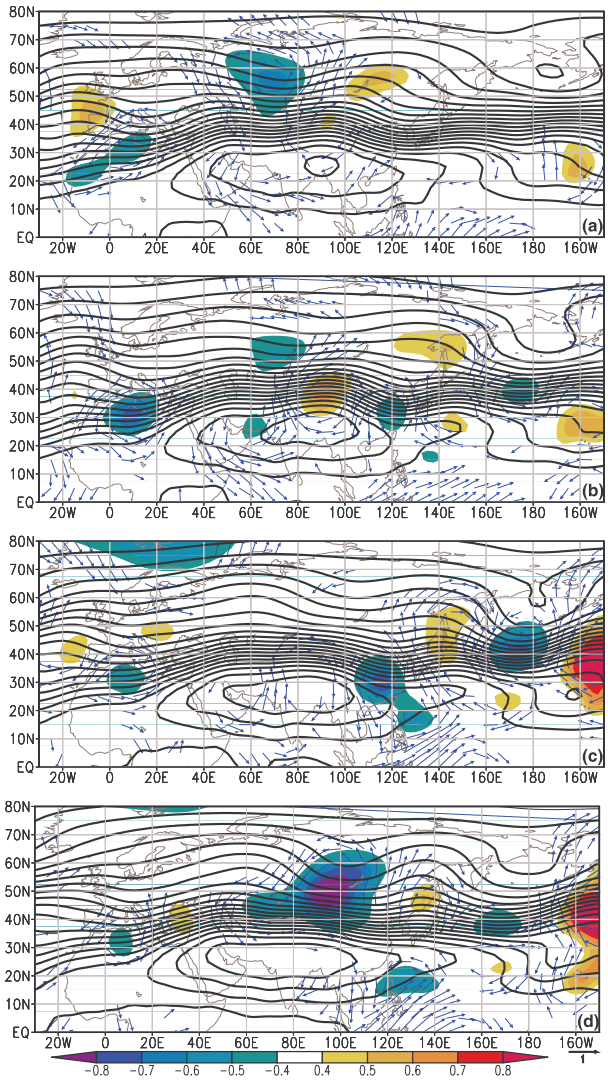

Fig. 7. Composite height (black contours with an interval of 40 m), height anomaly (shaded), and flow anomaly (vectors) for the 8 PHR events at 150 hPa on (a) day−13, (b) day−10, (c) day−7, and (d) day−4. Absolute magnitudes of height anomalies above 0.4 are shaded. Absolute magnitudes of normalized zonal and meridional flow anomalies significant above 0.4 are plotted.

It is this modulation that results in the buildup of favorable large scale circulation over Eurasia and the western North Pacific, as shown in Fig. 8. Figure 8 clearly shows the time evolution of the phase-lock condition in different stages linked to the Rossby wave train. Accompanying the pair of upper level height anomalies over Eurasia, the eastern part of the SAH extends northward first (Fig. 8a). Then, during the period from day−11 to day−8, both the SAH and SWPH intensify with the development of an anomalous low over southeastern China. It is obvious in Fig. 8b that the upper level northwesterly flow on the east flank of the SAH and southwesterly flow on the west flank of the SWPH intensify due to the development of the anomalous low. At the same time, a favorable westerly jet starts to establish over central Asia. With the further enhancement of the SAH and SWPH, the former extends eastward past 110°E at day−3 and the latter westward past 120°E at day−5 (Fig. 6b). Thus, the monsoon circulation cell mentioned above is created. Additionally, the favorable westerly jet intensifies because of the strong development of the long wave trough over the Baikal at day−4 (Fig. 8c).

In short, the facts revealed by the "one point" correlation maps and composites of the eight PHR events may suggest that the Rossby wave activity tied to the anomalous convection over the tropical Indian and maritime continent is an important mechanisms for conveying the anomalous impacts from the tropical oceans to the mid and high latitudes, even on the pentad time scale.

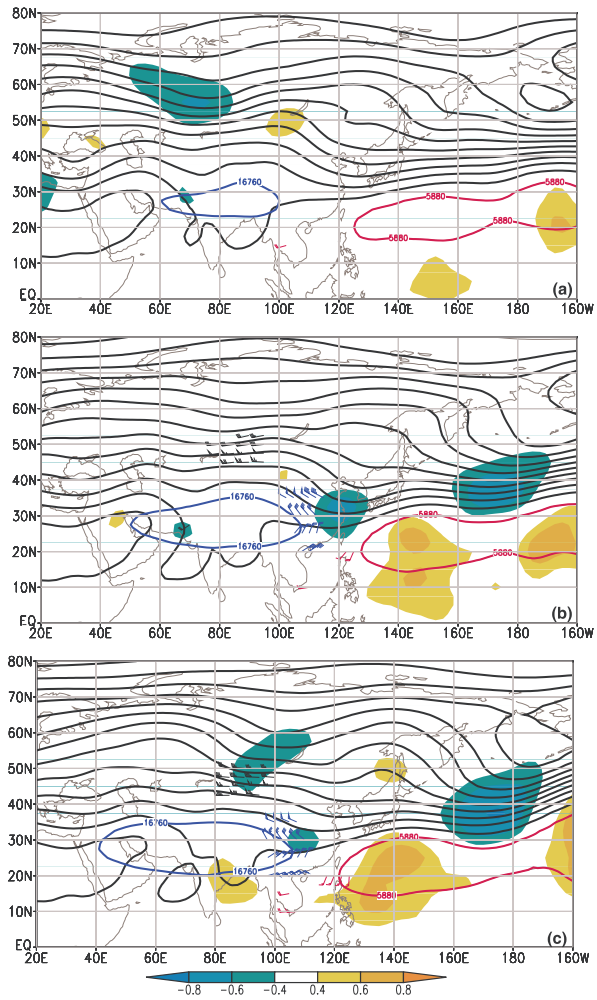

Fig. 8. Same as in Fig. 3 but for different time periods, (a) from day−15 to day−12; (b) from −11 to day−8, and (c) from day−7 to day−4.

3.4.3 *The critical variation of the SWPH for the onset of PHR events*

The SWPH is a very important circulation feature for the PHR events over the study area. Its variation in strength and position is greatly influenced by convective activity over the tropical oceans (Wang, 1994; Samel et al., 1999; Wang et al., 2001; Ding, 2005; Ding and Chan, 2005; Ding and Wang, 2005). It has been noted earlier in this study that suppressed convection clusters over the maritime continent and the tropical western Pacific abruptly jump northward three times when the east-suppressed/west-enhanced anomalous convection pattern shifts eastward with time before the PHR events (Figs. 1 and 2). After every northward jump, a prominent westward propagation of the significantly suppressed convection center follows. These changes may indicate the behavior of the SWPH before the PHR events.

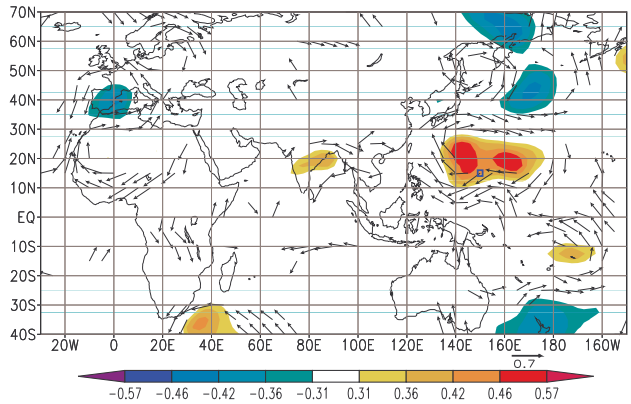

Fig. 9. "One point" correlation map showing the correlation coefficient between the OLR at a base point (shown as blue rectangle) and the pentad averaged height as well as wind fields at 500 hPa for the third pentad of June from 1974 to 2004. The values above the 90% statistical confidence level are shaded for height and plotted for wind vectors.

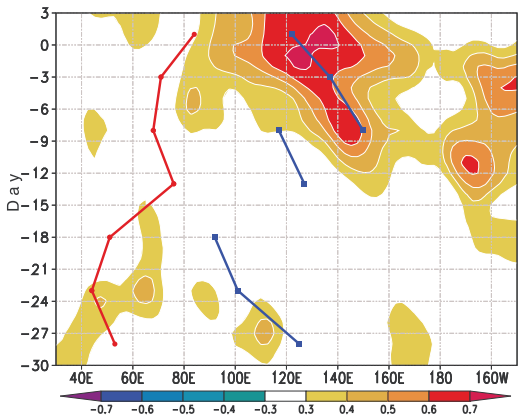

Fig. 10. Time-longitude plot of composite normalized height anomalies averaged between 10°N and 30°N at 500 hPa for the eight PHR events. The blue squares and red circles as well as the connecting lines between them have the same meanings as in Fig. 1.

Figure 9 is a "one point" correlation map for the third pentad of June (approximately the period from day−10 to day−6) at the level of 500 hPa. It can be seen from Fig. 9 that significant flow components and height manifest in an anti-cyclonic flow with positive height anomaly just around the suppressed convection center over the Philippine Sea. This indicates that there is a significant positive relationship between the suppressed convection over the Philippine Sea and the activity of the SWPH during mid June.

Figure 10 is a time-longitude plot of composite height anomalies averaged between 10°N and 30°N at 500 hPa for the 8 PHR events. Combining the information from Figs. 1 and 10, it is derived that significant

height anomalies match well with the suppressed convection centers over the Philippine Sea from day−7 to day+1. Therefore, it can be deduced that the northward jump and westward propagation of suppressed convection centers is consistent with the northward expansion and westward ridging of the SWPH before the PHR events. Furthermore, as mentioned above, the most direct influence from the anomalous convective activities with the east-suppressed/west-enhanced pattern over the tropical Indian and western North Pacific Oceans is the variation in anomalous zonal flow in the lower and mid troposphere. As shown in Fig. 5, a significant composite negative anomaly of zonal flow shifts eastward in the lower troposphere with the eastward shift of the pair of anomalous convection centers. Climatologically, easterly flow prevails over the area east of 140°E. Thus, the negative anomaly of that area from day−15 onward indicates the enhancement of easterly flow on the south and southwestern periphery of the SWPH, which certainly favors the intensification of the SWPH.

In summary, the northward expansion and westward ridging of the SWPH prior to the PHR events is directly or indirectly influenced by the anomalous convection over the tropical Indian Ocean, maritime continent, and Philippine Sea. More specifically, the direct influence comes from the altering of the local 3-D flow responding to the anomalous convective activity, as mentioned above. The indirect influence comes from the modulation of the large scale background due to the dispersion of the Rossby wave train over Eurasia.

4. Conclusions

Based on the NOAA daily satellite dataset of global OLR and daily precipitation observations for 743 surface weather stations for the period of 1974–2004, as well as NCEP/NCAR reanalysis from 1971 to 2004, the linkages between PHR events in the vicinity of the Yangtze River valley and the global OLR in the preceding 30 days was investigated by lag correlation and composite analyses. The main conclusions are summarized as follows.

There is a significant connection between the initiation of PHR events over the study area and anomalous convective activity, which is denominated by signals in this study over the tropical Indian Ocean, maritime continent, and tropical western Pacific Ocean. During the 30-day period prior to the onset of PHR events, the major anomalous convective centers have an apparent dipole structure, always with significant negative SOLRA denoting enhanced convection in the west, and significant positive SOLRA denoting suppressed convection in the east. This dipole structure continuously shifts eastward with time during the 30-day period. The enhanced convection mainly clusters over the tropical western Indian Ocean with slow shifting eastward of the significant negative SOLRA centers during the period. On the other hand, the suppressed convection occurs over a much broader area, from the eastern Indian Ocean to the maritime continent and Philippine Sea, in three clusters of east-west orientation. These three clusters appear in turn from the south to north with time. Within each of these clusters, significant positive SOLRA centers move westward.

The anomalous coherent changes in the convection pattern over the Asian summer monsoon domain have substantial impacts on the general circulation. With the eastward propagation of the dipole structure, an anomalous transverse circulation cell with westerly flow in the upper levels and easterly flow in the lower levels also shifts eastward. Therefore, the Walker circulation cell over the tropical Indian Ocean weakens. A direct consequence of the weakening Walker cell is the occurrence of a weak ISM condition, which favors the initiation of PHR events according to a number of previous works. Furthermore, when the dipole structure of anomalous convective activity over the tropical oceans moves eastward, the suppressed convection cluster shifts northward. Thus, the anomalous lower level easterly flow greatly favors the northward expansion and westward ridging of the SWPH, and therefore, favors the buildup of a condition of a phase-lock among large scale circulation features for the PHR events over the study area.

The most salient feature demonstrated in both of the "one point" correlation maps and the composite anomaly circulation fields is the signatures of a significant Rossby wave train in the mid to upper troposphere. Its passage is accompanied by the development of an anomalous trough over the vicinity of the Aral Sea, which is significantly related to the anomalously enhanced convection over the Indian Ocean southwest of the Indochina Peninsula during the third pentad of June (approximately from day−15 to day−11). It is the dispersion of this Rossby wave train that follows major modulation of the large scale circulation background, and occurs about two weeks before the buildup of a phase-lock condition favoring PHR events over the study area.

With the southeastward dispersion of this Rossby wave train, a trough over southeast China and upstream and downstream ridges develop, which causes the northward expansion of the SAH and SWPH. Then, after the disappearance of the Rossby wave train, the anomalous low over Southeast China weak-

ens, and the SAH extends eastward and the SWPH ridges westward. The upper level strong northwesterlies on the east flank of the SAH extend eastward and the lower level southwesterly jet on the southwest periphery of the SWPH extends westward, thus triggering the monsoon circulation cell over the study area. At the same time, a long wave trough develops over the Baikal, which favors the enhancement and eastward shift of the upper level westerly jet, as well as the buildup of a dual blocking pattern in the mid to high latitudes. Therefore, a favorable environment for the large scale phase-locking condition is established after the modulation of the large scale circulation associated with the excitation and dispersion of the Rossby wave train over Eurasia.

We realize that this is only a preliminary analysis, in which the connections between the anomalous convection over the tropical Indian Ocean and maritime continent and the PHR events are revealed with reasonable evidence. More studies are needed to demonstrate the robustness of the results obtained. As we know, the global to regional influences on the initiation and evolution of the PHR events over the study area are very complicated. We are optimistic that the facts revealed by this study will provide clues and motivation for future study.

Acknowledgements. NCEP reanalysis data used in this study was provided by the NOAA-CIRES Climate Diagnostics Center, Boulder, Colorado, USA, from their Web site at http://www.cdc.noaa.gov. The authors appreciate two anonymous reviewers' valuable comments on an early version of the manuscript, which led to significant improvement. This work was supported by the National Natural Science Foundation of China under Grant No. 40575015.

REFERENCES

Annamalai, H., and J. M. Slingo, 2001: Active/break cycles: Diagnosis of intraseasonal variability of the Asian Summer Monsoon. *Climate Dyn.*, **18**, 85–102.

Chelliah, M., and P. A. Arkin, 1992: Large-scale interannual variability of monthly outgoing longwave radiation anomalies over the global tropics. *J. Climate*, **5**, 371–389.

Ding, Q., and B. Wang, 2005: Circumglobal teleconnection in the Northern Hemisphere summer. *J. Climate*, **18**, 3483–3505.

Ding, Q., and B. Wang, 2007: Intraseasonal teleconnection between the summer Eurasian wave train and the Indian monsoon. *J. Climate*, **20**, 3751–3767.

Ding, Y., 2005: *Advanced Synoptic Meteorology.* China Meteorological Press, 585pp.

Ding, Y., and J. C. L. Chan, 2005: The East Asian summer monsoon: An overview. *Meteor. Atmos. Phys.*, **89**, 117–142.

Gruber, A., and A. F. Krueger, 1984: The status of the NOAA outgoing longwave radiation data set. *Bull. Amer. Meteor. Soc.*, **65**, 958–962.

Heddinghause, T. R., and A. F. Krueger, 1981: Annual and interannual variations in outgoing longwave radiation over the tropics. *Mon. Wea. Rev.*, **109**, 1208–1218.

Iwao, K., and M. Takahashi, 2008: A precipitation seesaw mode between northeast Asia and Siberia in summer caused by Rossby waves over the Eurasian Continent. *J. Climate*, **21**, 2401–2419.

Jiang, S. C., X. F. Yang, G. Wei, and W. B. Yang, 1993: The characteristics of "OLR" for 1991 Mei-Yu. *Quarterly Journal of Applied Meteorology*, **4**, 301–309. (in Chinese)

Jiang, S. C., and J. S. Winston, 1989: The characteristics of outgoing longwave radiation related to flood and drought over the Yangtze River Basin. *Acta Meteorologica Sinica*, **47**, 479–483. (in Chinese)

Lau, K. M., and M. T. Li, 1984: The monsson of East Asia and its global associations—a survey. *Bull. Amer. Meteor. Soc.*, **65**, 114–125.

Lau, K. M., and P. H. Chan, 1983: Short-term climate variability and atmospheric teleconnections from satellite-observed outgoing longwave radiation. I. Simultaneous relationship. *J. Atmos. Sci.*, **40**, 2735–2750.

Lawrence, D., and P. Webster, 2002: The boreal summer intraseasonal oscillation: Relationship between northward and eastward movement of convection. *J. Atmos. Sci.*, **59**, 1593–1606.

Livezey, R., and W. Chen, 1983: Statistical field significance and its determination by Monte Carlo techniques. *Mon. Wea. Rev.*, **111**, 46–59.

Li, Y., Y. Luo, and Y. Ding, 2004: The relationships between the global satellite-observed outgoing longwave radiation and the rainfall over China in summer and winter. *Advances in Space Research*, **33**, 1089–1097.

Li, Y. H., and Y. Liu, 1990: A preliminary analysis on the relationship between outgoing longwave radiation and drought/flood over North China. *Quarterly Journal of Applied Meteorology*, **2**, 213–217. (in Chinese)

Pierrehumbert, R., and R. Benestad, 2006: On a weakening of the Walker circulation. [Available online from http://www.realclimate.org/index.php/archives/2006/06/on-a-weakening-of-the-walker-circulation.]

Samel, A. N., W.-C. Wang, and X. Liang, 1999: The monsoon rainband over China and relationships with the Eurasian circulation. *J. Climate*, **12**, 115–131.

Shapiro, M. A., and A. J. Thorpe, 2002: THORpex Program Overview. [Available online from http://www-angler.larc.nasa.gov/thorpex/docs/thorpex_plan13.pdf]

Shi, N., F. Y. Wei, G. L. Feng, and T. L. Sheng, 1997: Monte Carlo test used in correlation and composite analysis of meteorological fields. *Journal of Nanjing Institute of Meteorology*, **20**, 355–359. (in Chinese)

Shi, N., and S. M. Zhu, 1991: Low frequency oscillation of OLR over tropics during spring and its relationship with persistent rainy period in kiddle and lower reaches of Yangtze River. *Chinese J. Atmos. Sci.*, **15**, 53–61. (in Chinese)

Tang, Y. B., J. J. Gan, L. Zhao, and K. Gao, 2006: On the climatology of persistent heavy rainfall events in China. *Adv. Atmos. Sci.*, **23**, 678–692.

Wang, B., 1994: Climate regimes of tropical convection and rainfall. *J. Climate*, **7**, 1109–1118.

Wang, B., and X.-H. Xu, 1997: Northern hemisphere summer monsoon singularities and climatological intraseasonal oscillation. *J. Climate*, **10**, 1071–1085.

Wang, B., R. Wu, and K.-M. Lau, 2001: Interannual variability of the Asian summer monsoon: Contrasts between the Indian and the Western North Pacific-East Asian monsoons. *J. Climate*, **14**, 4073–4090.

Xie, P.-P., and P. A. Arkin, 1998: Global monthly precipitation estimates from satellite-observed outgoing longwave radiation. *J. Climate*, **11**, 137–164.

Zhang, S. L., S. Y. Tao, Q. Y. Zhang, and J. Wei, 2002: Multi-scale circulation conditions of heavy rainfall in the middle and lower ranges of the Yangtze River basin. *Chinese Science Bulletin*, **47**, 467–473. (in Chinese)